Korean J. Chem. Eng., **31**(2), 343-349 (2014)
DOI: 10.1007/s11814-013-0244-z

pISSN: 0256-1115
eISSN: 1975-7220

Poly(ethyleneimine) functionalized organic-inorganic hybrid silica by hydrothermal-assisted surface grafting method for removal of nickel(II)

Lu He, Bing-Bing Wang, Dan-Dan Liu, Ke-Sen Qian, and Hong-Bo Xu†

College of Chemical Engineering, University of Science and Technology Liaoning, Anshan 114051, China
(*Received 7 August 2013 • accepted 19 November 2013*)

Abstract−Poly(ethyleneimine)-functionalized organic-inorganic hybrid silica adsorbent was synthesized by hydrothermal-assisted surface grafting technique for the removal of Ni(II) ions from aqueous solution, and was characterized by FT-IR, nitrogen adsorption and the static adsorption-desorption experiment method. The results indicated that the maximum static adsorption capacity of Ni(II) on poly(ethyleneimine)-functionalized hybrid silica adsorbent by hydrothermal heating method was 1.6 times as much as the conventional heating method. The poly(ethyleneimine)-functionalized hybrid silica adsorbent offered a fast kinetics for the adsorption of Ni(II), had a substantial binding capacity in the range of pH 4-8 and could be used repeatedly. The Langmuir adsorption model was more favorable than the Freundlich and Dubinin-Radushkevich adsorption models. The adsorption followed a pseudo-second-order model compared with pseudo-first-order model. Various thermodynamic parameters such as ΔG^o, ΔH^o and ΔS^o indicated that the adsorption process was spontaneous and endothermic. The results showed that poly(ethyleneimine)-functionalized hybrid silica adsorbent could be employed as an effective material for the removal of Ni(II) ions from aqueous solution.

Keywords: Nickel, Poly(ethyleneimine), Hydrothermal-assisted, Organic-inorganic Hybrid, Removal

INTRODUCTION

Nickel (Ni) use is widespread with industrial processes such as electroplating, plastics manufacturing, nickel-cadmium batteries, fertilizers, pigments, mining and metallurgical, porcelain enameling, copper sulfate manufacture and steam-electric power plants being the major contributors of Ni to the environment [1,2]. Ni is one of the toxic heavy metals that can be toxic to organisms, including humans, even at low concentrations [3,4] and hence, is graded as toxic pollutant, mutagenic agent and carcinogen by the EPA [5].

Over the last few decades, the main techniques developed for the removal of Ni(II) ions from aqueous solution include chemical precipitation [6], coagulation [7], ion exchange [8], membrane processing [9], solvent extraction [10] and electrochemistry method [11]. However, most of these techniques are expensive, require high expertise and produce toxic by-products as well [12]. Among these, adsorption is considered to be very important because of its cost effective treatment, easy operation, narrow space for plant siting, and no sludge produced [13]. The need for low operational cost, effective and regenerable adsorbents which are capable of removing Ni(II) ions from wastewater has received a great deal of interest.

The selection of an effective and economic adsorbent for removal of Ni(II) ions requires consideration of both conventional and unconventional materials such as siliceous materials [14], microorganisms [15], rice husk ash [16], bentonite clay [17], zeolite [18], carbon materials [19], sand [20] and metal oxide [21]. In recent years, silica gel has attracted considerable attention and is used as the support for the preparation of organic-inorganic hybrid materials due to its high specific surface area and excellent thermal and mechanical stability [22]. The chemical modification of silica gel has shown great promise in improving the efficiency of adsorption due to the increase of functional groups [23]. Poly(ethyleneimine) (PEI) is a typical alkaline water-soluble functional macromolecular which contains a large quantity of N-donor atoms and can react with Ni(II) ion [24-26]. The hydrothermal process is also a promising method for the synthesis of advanced materials, and receives much attention due to the simple, high sample throughput, a small amount of reagent volume, reliable temperature and pressure control, and suitable reaction temperature [27,28]. However, the PEI-functionalized organic-inorganic hybrid silica by the hydrothermal-assisted surface grafting method for the removal of Ni(II) from aqueous solution has not been reported.

We prepared a PEI-functionalized organic-inorganic hybrid silica by the hydrothermal-assisted surface grafting method and used it as an effective adsorbent for the removal of Ni(II) ion from aqueous solution. The adsorption behavior of Ni(II) ion on the PEI-functionalized organic-inorganic hybrid silica was investigated. Thermodynamic study was also evaluated.

EXPERIMENTAL

1. Reagents

3-Chloropropyltriethoxsilane was purchased from Jingzhou Jinghan Fine Chemical Co., Ltd. Hubei, China. Branched poly (ethyleneimine) (PEI) (molecular weight of 25,000) was obtained from Sigma-Aldrich. Silica gel (60-80 mesh) was purchased from Qingdao Ocean Chemical Co., Ltd., Shandong, China. All the reagents were of analytical grade and purchased from Sinopharm Chemical Reagent Co., Ltd. Shanghai, China. Deionized water was used throughout.

2. Apparatus

The Fourier transmission infrared spectra (FT-IR) of the samples in KBr pellets were performed by a Nicolet 6700 FT-IR spectrom-

†To whom correspondence should be addressed.
E-mail: lnkdxhb@163.com

eter in the range from 4,000 to 400 cm^{-1} with a resolution of 1 cm^{-1}. The surface area of the sample particles synthesized was determined using a porosimetry analyzer (ASAP 2010C, Micromeritics, USA) in the Brunauer-Emmett-Teller (BET) model. The samples were degassed and dried before this measurement. The concentrations of metals in aqueous solutions were determined by an AA-6300c flame atomic absorption spectrometer (FAAS, Shimadzu Corporation, Japan) with Ni hollow cathode lamps and air-acetylene flame after appropriate dilutions and acidification to pH~2 adjusted with HNO_3. The hollow cathode lamp was operated at 15 mA and the analytical wavelength was set at 232 nm. The pH of solution was measured by a pHS-3C digital pH meter equipped with a combined electrode (Shanghai Precision & Scientific Instrument Co., LTD, Shanghai, China). The pH was maintained in the range of ±0.1 U until equilibrium was attained.

3. Synthesis and Characterization of PEI-functionalized Hybrid Silica Adsorbent

The PEI-functionalized hybrid silica adsorbent was prepared according to the steps described in Ref. [29]. First, 6 g of silica gel particles was treated for activating by refluxing in 60 mL of 33% solution of methanesulfonic acid as an activation reagent with stirring for 8 h. Second, 4 g of activated silica gel reacted with chloropropyltriethoxsilane using xylene as solvent by the hydrothermal reaction in a Teflon-lined stainless steel autoclave at 120 ºC for 24 h or by conventional heating at 80 ºC for 24 h. Third, 10 mL of 10% PEI aqueous solution was added, and then reaction was performed in a Teflon-lined stainless steel autoclave at 120 ºC for 24 h or by conventional heating at 80 ºC for 24 h. Finally, the solid prepared was filtered, washed by ethanol and water (pH≈7), and dried in vacuum at 60 ºC for 12 h. The chemical structure of the solid prepared after grafting was characterized by infrared spectrum to confirm that PEI had been grafted onto the surface of silica gel particle. The surface areas of the sample particles synthesized and silica gel particles were determined. The amino concentration of the sample particles synthesized was determined by acid-base titration analysis [30,31].

4. Static Adsorption Experiments

Adsorption studies were conducted at varied adsorption concentration (50-600 mg·L^{-1}), adsorption time (5-60 min), and temperature (25, 35 and 45 ºC). The effect of the medium pH on the adsorption capacity was also investigated in batch adsorption equilibrium experiments in the pH range 2-9 at 25 ºC. In all the experiments, PEI-functionalized hybrid silica concentration was kept constant at 100 mg/25 mL. The suspensions were brought to the desired pH by adding sodium hydroxide and hydrochloric acid.

The uptake of Ni(II) ions was calculated by the simple concentration difference method. The metal uptake Q (mg Ni(II) adsorbed/g adsorbent) was calculated from the mass balance equation (Eq. (1)) as follows:

$$Q = \frac{(C_i - C_f)V}{1000\ W} \quad (1)$$

where C_i and C_f are the initial and final concentrations of Ni(II) ions (mg·L^{-1}), respectively. V is the volume of the solution (mL); W is the mass used of adsorbents (g).

5. Desorption and Repeated Reuse of PEI-functionalized Hybrid Silica Adsorbent

To evaluate the desorption ratio, the adsorbed Ni(II) ions were desorbed by the treatment with 1 mol·L^{-1} HCl solution. The adsorbents were placed in the desorption medium and stirred continuously for 2 h. The final concentrations of Ni(II) ions in the aqueous phase were determined by FAAS. The desorption ratio was calculated as follows:

$$\text{Desorption ratio (\%)} = \frac{\text{amount of Ni(II) ions desorbed to the elution medium (mg)}}{\text{amount of Ni(II) ions adsorbed onto the adsorbent (mg)}} \times 100 \quad (2)$$

The adsorption/desorption cycle was performed up to five times to evaluate the possibility of repeated reuse of PEI-functionalized hybrid silica adsorbent. The Ni(II) ions were removed from the adsorbents by washing with 1 mol·L^{-1} HCl for 2 h. The adsorbents were rinsed several times with deionized water and dried under vacuum at 60 ºC overnight before another cycle. The adsorption ratio of each cycle was calculated as a percentage of the uptake at the first adsorption.

For all samples, the data represented the mean of three independent experiments. Confidence intervals of 95% were calculated for each set of samples to determine the margin of error. For each set of data present, standard statistical methods were used to determine the mean values and standard deviations. All statistical analysis was done using Microsoft Excel 2003, Version office XP.

RESULTS AND DISCUSSION

1. Characterization

To confirm the presence of PEI in the functionalized silica gel adsorbents, the FT-IR spectra of silica gel and PEI-functionalized hybrid silica are shown in Fig. 1 and the results are shown in Table 1. The absorption bands at 3,629-3,731 cm^{-1} and 1,701 cm^{-1} are the stretching vibration and bending vibration of N-H bond, respectively. The absorption band at 3,440 cm^{-1} is attributed to stretching vibration of O-H groups on the surface silanol groups with hydrogen bond and the remaining adsorbed water molecules. The absorption band at 1,653 cm^{-1} is due to the deformation vibrations of adsorbed water molecules. The absorption bands at 2,933 and 2,857 cm^{-1} are ascribed to the asymmetric stretching vibrations of -CH_2- groups, while the absorption peaks at 1,444 and 1,409 cm^{-1} are related to the bending vibrations of -CH_2- groups. The band at 1,560

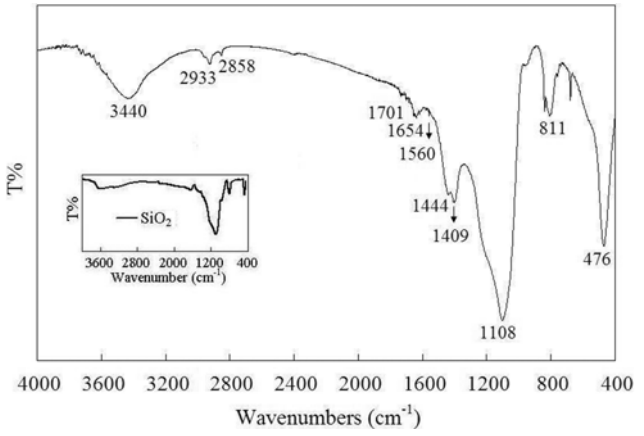

Fig. 1. IR spectra of silica gel and PEI-functionalized hybrid silica adsorbents.

Table 1. IR parameters of PEI-functionalized hybrid silica

Wavenumbers (cm^{-1})	Type of vibration	Bonds
3629-3731	Stretching vibration	N-H bond
1701	Bending vibration	N-H bond
3440	Stretching vibration	O-H bond
1653	Deformation vibrations	O-H bond
2933 and 2857	Asymmetric stretching vibrations	$-CH_2$-bond
1444 and 1409	Bending vibrations	$-CH_2$-bond
1560	Stretching vibration	C-N bond
1108	Stretching vibrations	Si-O-Si bond
811	Stretching vibrations	Si-O bond
476	Bending vibrations	Si-O-Si bond

cm^{-1} is the stretching vibration absorption of C-N bond. The absorption bands at 1,108 cm^{-1} and 811 cm^{-1} are due to the Si-O-Si and Si-O stretching vibrations, respectively. The absorption peak at 476 cm^{-1} is assigned to the bending vibrations of Si-O-Si groups. Compared with the silica gel, PEI-functionalized hybrid silica had more bands. These indicated that PEI had been successfully grafted on the surface of silica after modification. Similar results were reported previously [32].

The content of amino groups onto PEI-functionalized hybrid silica by hydrothermal heating and by conventional heating was 5.2% and 3.1% due to the improvement of grafting efficiency through reliable temperature and pressure control of hydrothermal heating.

BET surface areas of silica gel, PEI-functionalized hybrid silica by hydrothermal heating and PEI-functionalized hybrid silica by conventional heating were 122, 75 and 64 $m^2 \cdot g^{-1}$, respectively. The surface area of PEI-functionalized hybrid silica adsorbents was dramatically reduced with the increase of the grafting efficiency of PEI because the silylation covered the pore openings on the surface of silica [22]. The surface area of PEI-functionalized hybrid silica by hydrothermal heating was less than that of PEI-functionalized hybrid silica by conventional heating because more PEI had been grafted to the surface of silica.

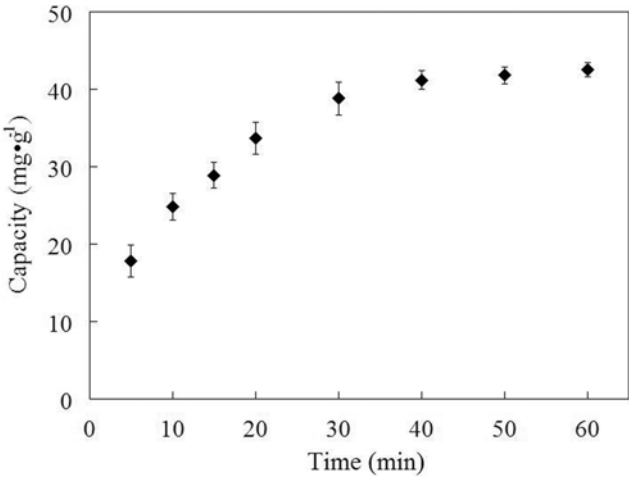

Fig. 2. Effect of contact time on the adsorption equilibrium for Ni(II): Concentration of Ni(II)=400 mg·L^{-1}, pH=5, temperature=25 °C.

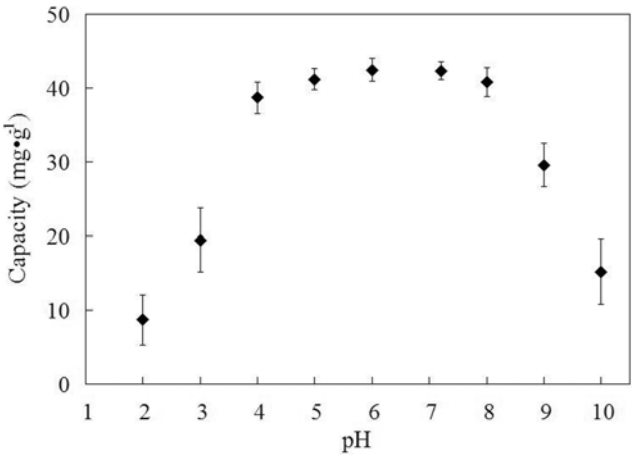

Fig. 3. Effect of pH on the adsorption capacity of PEI-functionalized hybrid silica adsorbent for Ni(II): Concentration of Ni(II) =400 mg·L^{-1}, time=45 min, temperature=25 °C.

2. Effect of Contact Time

The effect of contact time on adsorption of Ni(II) ions by PEI-functionalized hybrid silica was investigated from 5 to 60 min as shown in Fig. 2. Results showed that adsorption of Ni(II) ions was dependent on different time intervals adsorption and took place in two stages: a very rapid surface adsorption and a slow intracellular diffusion. Kinetic studies revealed that maximum adsorption capacity for Ni(II) ions was achieved generally in the first 30 min, adsorption took place very rapidly, and then continued at slower rate up to maximum adsorption capacity. A contact time of 45 min was enough as the equilibration time for the further experiments.

3. Effect of pH

The solution pH is an important parameter that influences most adsorption systems. The effect of the pH on the adsorption capacity of Ni(II) ions onto PEI-functionalized hybrid silica is shown in Fig. 3. Results indicated that the pH strongly influenced the binding of Ni(II) ions on the surface of PEI-functionalized hybrid silica adsorbent. At low pH (pH<4), a lower adsorption capacity of Ni(II) was obtained because the interaction of adsorbent binding sites with protons restricted the approach of Ni(II) ions. With increase in pH, more negatively charged surface attracted more positively charged Ni(II) ions for binding resulting in the higher adsorption capacity of Ni(II) ions. Small amount of Ni(II) uptake was bound at pH>8 due to the formation of Ni(II) hydroxide precipitation. The effective pH range of PEI-functionalized hybrid silica for Ni(II) ions was 4-8, so pH 5 was considered to be the optimum pH for the further studies.

4. Adsorption Capacity

As can be seen in Fig. 4, the amount of Ni(II) adsorbed per unit mass of PEI-functionalized hybrid silica by hydrothermal heating and conventional heating increased with the initial concentrations of Ni(II) ions till the plateau values (adsorption capacity values) were obtained. This adsorption characteristic indicated that the surface saturation was dependent on the initial concentrations of Ni(II) ions. At low concentrations, adsorption sites take up the available metal more quickly. However, at higher concentrations, Ni(II) ions needing to diffuse to the surface of PEI-functionalized hybrid silica

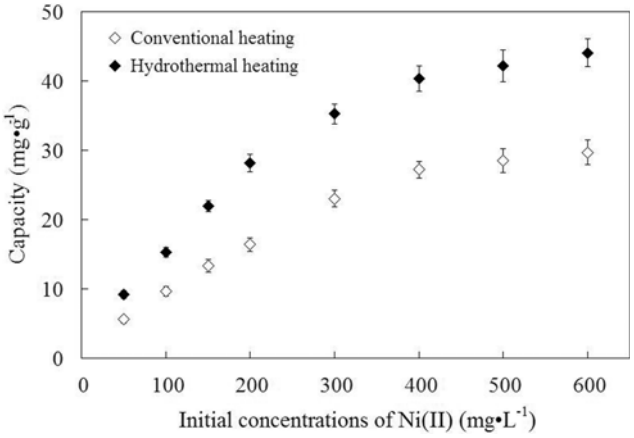

Fig. 4. Adsorption capacity of PEI-functionalized hybrid silica adsorbent for Ni(II): pH=5, time=45 min, temperature=25 °C.

by intraparticle diffusion and greatly hydrolyzing ions will diffuse at a slower rate. The maximum static adsorption capacities of Ni(II) on PEI-functionalized hybrid silica by hydrothermal heating were calculated as 42.2 $mg \cdot g^{-1}$, and were 1.6 times as much as that by conventional heating (27.1 $mg \cdot g^{-1}$) because more PEI were grafted to the surface of silica by hydrothermal heating. This result was consistent with the results of BET and the content of amino groups onto PEI-functionalized hybrid silica.

Maximum adsorption capacities reported in the literature for adsorption of Ni(II) ions on different adsorbents were compared with the value for PEI-functionalized hybrid silica in this study. Although the direct comparison of PEI-functionalized hybrid silica with the other adsorbent materials was difficult, owing to the different experimental conditions, the maximum adsorption capacity of PEI-functionalized hybrid silica was higher than for the many adsorbents listed in Table 2 [17-21,33-38].

Table 3. Calculated kinetic parameters for the adsorption of Ni(II) onto PEI-functionalized hybrid silica adsorbent

Pseudo-first-order model	Pseudo-second-order model
k_1=0.0608 min^{-1}	k_2=2.22×10^{-3} $g \cdot mg^{-1} \cdot min^{-1}$
q_{eq} (cal)=29.9 $mg \cdot g^{-1}$	q_{eq} (cal)=48.5 $mg \cdot g^{-1}$
r^2=0.9711	r^2=0.9980

5. Adsorption Kinetics

Adsorption kinetic studies were conducted to understand the kinetic behavior of PEI-functionalized hybrid silica toward Ni(II) ions. Parameters from two kinetic models, pseudo-first-order [39] and pseudo-second-order [40], were fit to experimental data to examine the adsorption kinetics of metals uptakes by PEI-functionalized hybrid silica.

The linear form of pseudo-first-order-model can be expressed as:

$$\lg(q_e - q_t) = \lg q_e - k_1 t/2.303 \quad (3)$$

where k_1 (min^{-1}) is the rate constant of the pseudo-first-order adsorption. q_e and q_t ($mg\ g^{-1}$) are the adsorption capacities at equilibrium and at time t (min), respectively. The rate constants k_1, q_e and correlation coefficients r^2 were calculated using the slope and intercept of plots of $\lg(q_e - q_t)$ versus t.

The pseudo-second-order rate expression is linearly expressed as:

$$t/q_t = 1/k_2 q_e^2 + t/q_e \quad (4)$$

where q_e and q_t are the adsorption capacity at equilibrium and time t ($mg \cdot g^{-1}$), k_2 ($g \cdot mg^{-1} \cdot min^{-1}$) is the rate constant of the pseudo-second-order adsorption. The rate constants k_2, q_e and correlation coefficients r^2 were calculated from the linear plots of t/q_t versus t.

Table 3 lists the calculated results and the correlation coefficients (r^2). The r^2 of the pseudo-first-order kinetic and pseudo-second-order models was 0.9711 and 0.9980, respectively. The r^2 of the pseudo-second-order kinetic model was very close to 1. Also, the calculated

Table 2. Comparison of the maximum adsorption capacity of various adsorbents toward Ni(II) ions from the literature

Adsorbents	Capacity ($mg \cdot g^{-1}$)	Ref.
Bofe bentonite clay	1.9	[17]
Iranian natural zeolite	3.4	[18]
Oxidized multi-walled carbon nanotubes	49.3	[19]
Modified riverbed sand	0.86	[20]
Silico-titanate	6.0	[21]
Silico-antimonate	2.0	[21]
Red mud	13.7	[31]
Calcined phosphate	15.5	[31]
Clarified sludge	14.3	[31]
Escherichia coli biosorbent	26.5	[32]
Punica granatum peel waste	52.0	[33]
Granular activated carbon	2.9	[34]
Granular activated carbon modified with potassium bromate	5.8	[34]
Peat	8.8	[35]
Natural neem (*Azadirachta indica*) sawdust	31.5	[36]
Acid treated neem (*Azadirachta indica*) sawdust	74.1	[36]
PEI-functionalized hybrid silica	42.2	This study

Table 4. Isotherms parameters for the adsorption of Ni(II) by PEI-functionalized hybrid silica adsorbent

Langmuir adsorption isotherm	Freundlich adsorption isotherm	Dubinin-Radushkevich isotherm
q_{max}=52.4 mg·g^{-1}	K_F=2.99	k_{ad}=0.035 mol^2·kJ^{-2}
b=0.013 L·mg^{-1}	n=2.14	q_s=23.9 mg·g^{-1}
r^2=0.9959	r^2=0.9658	r^2=0.9885

q_e values obtained from the pseudo-first-order kinetic and pseudo-second-order kinetic models were 29.9 and 48.5 mg·g^{-1}, respectively. The calculated q_e values of pseudo-first-order kinetic model did not give reasonable values, which were low compared with experimental q_e value (42.2 mg·g^{-1}). Also, the calculated q_e value of pseudo-second-order kinetic model almost agreed with the experimental data. This indicated that the adsorption system of PEI-functionalized hybrid silica for Ni(II) ions belonged to the pseudo-second-order kinetic model. The results suggested that the adsorption of Ni(II) ions onto PEI-functionalized hybrid silica was mainly dominated by chemical adsorption reactions.

6. Adsorption Isotherms

The analysis of the isotherm data is important to develop an equation which accurately represents the results and can be used for design purposes [39]. Langmuir, Freundlich and Dubinin-Radushkevich isotherms were chosen to describe the adsorption process.

The Langmuir isotherm assumes monolayer adsorption onto a surface containing a finite number of adsorption sites of uniform adsorption with no transmigration of adsorbate in the plane of the surface. The linear expression of Langmuir adsorption isotherm can be described as Eq. (5) [42].

$$C_{eq}/q_{eq}=1/(q_{max}b)+C_{eq}/q_{max} \quad (5)$$

where q_{eq} is the amount of adsorbed metals in the adsorbent (mg·g^{-1}), C_{eq} is the equilibrium ion concentration in solution (mg·L^{-1}), b (L·mg^{-1}) is the equilibrium constant related to the adsorption energy, and q_{max} is the maximum adsorption capacity (mg·g^{-1}). A linear plot is obtained when C_{eq}/q_{eq} is plotted against C_{eq} over the entire concentration range of metal ions investigated.

The Freundlich isotherm assumes heterogeneous surface energies, in which the energy term in the Langmuir equation varies as a function of the surface coverage. The linear form of the Freundlich adsorption isotherm can be represented by Eq. (6) [43].

$$\log q_{eq}=\log k_F+(1/n)\log C_{eq} \quad (6)$$

where K_F and n are the Freundlich constants; C_{eq} is the equilibrium ion concentration in solution (mg·L^{-1}). According to Eq. (6), the values of K_F and n can be determined experimentally by plotting log q_{eq} versus log C_{eq}.

The Dubinin-Radushkevich isotherm is more general because it does not assume a homogeneous surface or constant adsorption potential [44]. It was applied to estimate the porosity apparent free energy and the characteristics of adsorption [45].

$$q_e=q_s \exp(-k_{ad}\varepsilon^2) \quad (7)$$

The linear form can be represented as

$$\ln q_e=\ln q_s-k_{ad}\varepsilon^2 \quad (8)$$

where, k_{ad} is the Dubinin-Radushkevich isotherm constant (mol^2·kJ^{-2}); q_s is the theoretical isotherm saturation capacity (mg·g^{-1}); q_e is the amount of adsorbate in the adsorbent at equilibrium (mg·g^{-1}); ε is Dubinin-Radushkevich isotherm constant and calculated as follows:

$$\varepsilon=RT\ln(1+1/C_e) \quad (9)$$

where, R is the universal gas constant (8.314 J·mol^{-1}K^{-1}); T the temperature (K); C_e the equilibrium concentration (mol·L^{-1}). The slope of the plot of ln q_e versus ε^2 gives k_{ad} and the intercept yields the adsorption capacity, q_s.

The experimental data are fitted by the Langmuir, Freundlich and Dubinin-Radushkevich isotherms and the values calculated from the three models are listed in Table 4. The linear regression coefficients (r^2) of Langmuir, Freundlich and Dubinin-Radushkevich isotherms were 0.9959, 0.9658 and 0.9885, respectively. The Langmuir isotherm model was slightly better than Freundlich isotherm and Dubinin-Radushkevich isotherm models to fit Ni(II) ions adsorption data well compared with r^2. There was a noted difference between the experiment value (42.2 mg·g^{-1}) and the theoretical value by Dubinin-Radushkevich isotherm model (23.9 mg·g^{-1}) of adsorption capacity. The Langmuir adsorption model was more favorable with a low difference between the experiment (42.2 mg·g^{-1}) and calculation (52.4 mg·g^{-1}) values of adsorption capacity. For adsorption data analysis, the Langmuir adsorption model was employed to describe the adsorption process of Ni(II) ions onto PEI-functionalized hybrid silica, indicating that the adsorption behavior of Ni(II) ions may be belong to monolayer adsorption.

7. Thermodynamic Study

The thermodynamic parameters can be determined from the thermodynamic equilibrium constant, K_0. The standard Gibbs free energy ΔG^o (kJ·mol^{-1}), standard enthalpy change ΔH^o (kJ·mol^{-1}), and standard entropy change ΔS^o (J·mol^{-1}·K^{-1}) can be estimated from changes of equilibrium constants as a function of temperature and are calculated using the following equations:

$$\Delta G^o=-RT\ln K_0 \quad (10)$$

$$\ln K_0=\frac{\Delta S^o}{R}-\frac{\Delta H^o}{RT} \quad (11)$$

R, the universal gas constant, 8.314 J·mol^{-1}·K^{-1}, and T is the solute temperature (K). K_0 can be defined as [46,47]:

$$K_0=\frac{a_s}{a_e}=\frac{\gamma_s C_s}{\gamma_e C_e} \quad (12)$$

where a_s is the activity of adsorbed metals, a_e is the activity of metals in solution at equilibrium, γ_s is the activity coefficient of adsorbed metals, γ_e is the activity coefficient of metals in equilibrium solution, C_s is the metals adsorbed on PEI-functionalized hybrid silica adsorbent (mmol g^{-1}), and C_e is the metals concentration in equi-

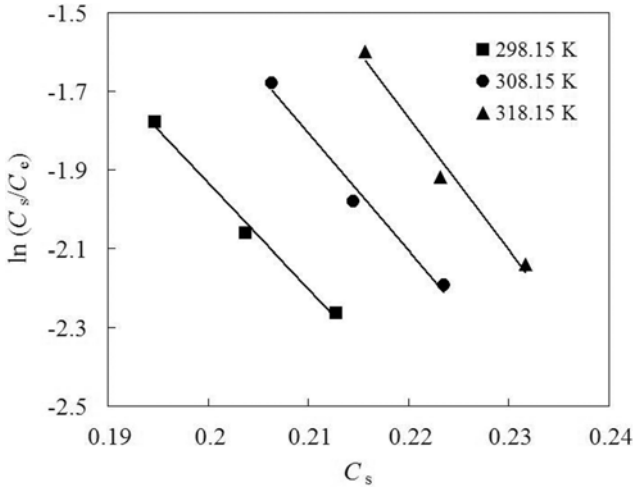

Fig. 5. Plots of ln(C_s/C_e) vs. C_s at various temperatures.

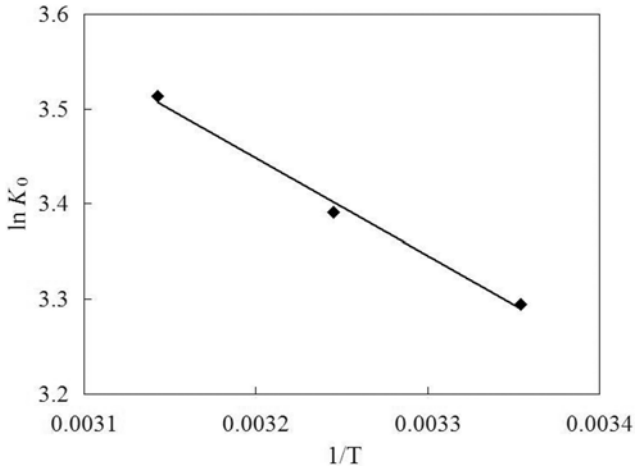

Fig. 6. Variation of equilibrium constant (K_0) as a function of temperature (1/T).

librium solution (mmol mL^{-1}). The expression of K_0 can be simplified by assuming that the concentration in the solution approaches zero, resulting in $C_s \rightarrow 0$ and $C_e \rightarrow 0$ and the activity coefficients approach unity at the every low concentration [46,47]. Eq. (12) can be written as:

$$C_s \xrightarrow{lim} 0 \frac{C_s}{C_e} = \frac{a_s}{a_e} = K_0 \quad (13)$$

K_0 at different temperatures was determined by plotting ln(C_s/C_e) versus C_s (Fig. 5) and extrapolating C_s to zero [46,47]. The straight line obtained was fitted to the points by least-squares analysis. Based on Eqs. (10) and (11), the values of ΔH^o and ΔS^o were calculated from the slope and intercept of linear plot of ln K_0 versus 1/T, respectively (as shown in Fig. 6).

Table 5 presents the thermodynamic parameters. The negative values of ΔG^o at all the experimental temperature indicate that the metal absorption by PEI-functionalized hybrid silica was spontaneous. The positive values of ΔH^o suggest the endothermic nature of the process. The positive value of entropy change (ΔS^o) of the system suggests an increase in disorder and randomness at the solid/solution interface during the adsorption of Ni(II) ions onto PEI-functionalized hybrid silica, while for the adsorption there were some structural changes in the Ni(II) ions and the adsorbent occur. The adsorbed water molecules, which were displaced by the Ni(II) ions, gained more translational entropy than were lost by the Ni(II) ions, thus allowing the increase of randomness in the system [48]. Similar adsorption systems were reported previously [49,50].

Table 5. Values of various thermodynamic parameters for adsorption of Ni(II) on PEI-functionalized hybrid silica adsorbent

Thermodynamic constants	Temperature (K)		
	298.15	308.15	318.15
K_0	26.98	29.71	33.55
ΔG^o (kJ·mol^{-1})	−8.17	−8.69	−9.29
ΔH^o (kJ·mol^{-1})		8.58	
ΔS^o (J·mol^{-1}·K^{-1})		56.12	

Table 6. Five stripping cycles of PEI-functionalized hybrid silica adsorbent

Stripping cycle	W (g)	Q (mg/g)	Adsorption ratio (%)
1	0.2000	40.5	-
2	0.1800	38.1	94.1
3	0.1600	36.9	91.1
4	0.1400	36.2	89.4
5	0.1200	35.6	87.9

8. Desorption and Regeneration

We also studied desorption of the adsorbed metals ions from PEI-functionalized hybrid silica in a batch experimental setup. When 1 mol·L^{-1} HCl solution was used as a desorption agent, Ni(II) ions were released from 0.5 g of PEI-functionalized hybrid silica into 25 mL of desorption medium. The desorption time was found to be 2 h and desorption ratios were very high (up to 95%).

Regeneration of any exhausted adsorbent is an important factor in the adsorption process for improving the process economics [51]. Regeneration allows for the repeated use of the adsorbent and decreasing costs. The same sample of the adsorbent was used for the adsorption of Ni(II) ions from solutions after five stripping cycles (as shown in Table 6). After the fifth adsorption/desorption cycle, the adsorption capacity of Ni(II) ions was found to about 88% of the fresh adsorbent. The results indicated that PEI-functionalized hybrid silica had good regeneration ability.

CONCLUSION

PEI-functionalized hybrid silica was successfully prepared by the hydrothermal assisted surface grafting technique. This method provided the simple reactive condition and improved the adsorption capacity of Ni(II) ions. The prepared PEI-functionalized hybrid silica exhibited good characteristics, such as fast adsorption kinetics, high adsorption capacity, and good regeneration ability. The kinetic data showed a well fitted pseudo-second-order kinetic model. The adsorption of Ni(II) ions on PEI-functionalized hybrid silica adsorbent followed the Langmuir model. Thermodynamic study

indicated that the adsorption process was endothermic and spontaneous. PEI-functionalized hybrid silica adsorbent is a promising adsorbent for the removal of Ni(II) ions from aqueous solution.

ACKNOWLEDGEMENTS

This work was sponsored by the Scientific Research Foundation of the Educational Department of Liaoning Province (grant no. L2012102), Administration Foundation of Science & Technology of Anshan, Liaoning Province (grant no. 2011MS13), and Special Foundation of University of Science and Technology Liaoning (grant no. 2012CX03).

REFERENCES

1. B. Volesky and Z. R. Holan, *Biotechnol. Prog.*, **11**, 235 (1995).
2. G. Selvakumari, M. Murugesan, S. Pattabi and M. Sathishkumar, *Bull. Environ. Contam. Toxicol.*, **69**, 195 (2002).
3. E. Erdem, N. Karapinar and R. Donat, *J. Colloid Interface Sci.*, **280**, 309 (2004).
4. Agency for toxic substances and disease registry, Toxicological profiles, US Department of Health and Human Services, Atlanta (1999).
5. D. H. Antonsen, *Encyclopedia of chemical technology*, Wiley, New York, 801 (1981).
6. A. K. Golder, V. S. Dhaneesh, A. N. Samanta and S. Ray, *Chem. Eng. Technol.*, **31**, 143 (2008).
7. S. Vasudevan, J. Lakshmi and G. Sozhan, *Environ. Sci. Pollut. Res.*, **19**, 2734 (2012).
8. S. Rengaraj, K.-H. Yeon and S.-H. Moon, *J. Radioanal. Nucl. Chem.*, **253**, 241 (2002).
9. M. Hebrant, A. Bouraine, A. Brembilla, P. Lochon and C. Tondre, *Colloid Polym. Sci.*, **273**, 598 (1995).
10. I. Mihaylov, *JOM*, **55**, 38 (2003).
11. K. N. Njau and L. J. J. Janssen, *J. Appl. Electrochem.*, **25**, 982 (1995).
12. R. Apiratikul and P. Pavasant, *Bioresour. Technol.*, **99**, 2766 (2008).
13. S. S. Bozkurt, Z. B. Molu, L. Cavas and M. Merdivan, *J. Radioanal. Nucl. Chem.*, **288**, 867 (2011).
14. I. Dahlan and M. H. M. Razali, *Water Air Soil Pollut.*, **223**, 2495 (2012).
15. M. D. Machado, H. M. V. M. Soares and E. V. Soares, *Water Air Soil Pollut.*, **212**, 199 (2010).
16. T. G. Chuah, A. Jumaisah, I. Azni, S. Katayan and C. S. Y. Thomas, *Desalination*, **175**, 305 (2005).
17. M. G. A. Vieira, A. F. Almeida Neto, M. L. Gimenes and M. G. C. da Silva, *J. Hazard. Mater.*, **177**, 362 (2010).
18. H. Merrikhpour and M. Jalali, *Clean Technol. Environ. Policy*, **15**, 303 (2013).
19. M. I. Kandah and J. L. Meunier, *J. Hazard. Mater.*, **146**, 283 (2007).
20. S. Yadav, V. Srivastava, S. Banerjee, F. Gode and Y. C. Sharma, *Environ. Sci. Pollut. Res.*, **20**, 558 (2013).
21. M. M. Abou-Mesalam, *J. Radioanal. Nucl. Chem.*, **252**, 579 (2002).
22. F. Hoffmann, M. Cornelius, J. Morell and M. Fröba, *Angew. Chem. Int. Ed.*, **45**, 3216 (2006).
23. P. K. Jal, S. Patel and B. K. Mishra, *Talanta*, **62**, 1005 (2004).
24. V. N. Kislenko and L. P. Oliynyk, *J. Polym. Sci., Part A: Polym. Chem.*, **40**, 914 (2002).
25. R. Say, A. Tuncel and A. Denizli, *J. Appl. Polym. Sci.*, **8**3, 2467 (2002).
26. S. Deng and Y.-P. Ting, *Water Res.*, **39**, 2167 (2005).
27. K. Byrappa and T. Adschiri, *Prog. Cryst. Growth Charact. Mater.*, **53**, 117 (2007).
28. H. Hayashi and Y. Hakuta, *Materials*, **3**, 3794 (2010).
29. B. Gao, P. Jiang and H. Lei, *Mater. Lett.*, **60**, 3398 (2006).
30. M. Sela and A. Berger, *J. Am. Chem. Soc.*, **77**, 1893 (1955).
31. M. A. Peters, A. M. Belu, R. W. Linton, L. Dupray, T. J. Meyer and J. M. De Simone, *J. Am. Chem. Soc.*, **117**, 3380 (1995).
32. B. Gao, X. Wang and Y. Shen, *Biochem. Eng. J.*, **28**, 140 (2006).
33. Y. Hannachi, N. A. Shapovalov and A. Hannachi, *Korean J. Chem. Eng.*, **27**, 152 (2010).
34. I. S. Kwak, S. W. Won, S. B. Choi, J. Mao, S. Kim, B. W. Chung and Y.-S. Yun, *Korean J. Chem. Eng.*, **28**, 927 (2011).
35. A. Bhatnagara and A. K. Minocha, *Colloids Surf. B*, **76**, 544 (2010).
36. D. Satapathy and G. S. Natarajan, *Adsorption*, **12**, 147 (2006).
37. Y. S. Ho and G. McKay, *Adsorption*, **5**, 409 (1999).
38. P. S. Rao, K. V. N. S. Reddy, S. Kalyani and A. Krishnaiah, *Wood Sci. Technol.*, **41**, 427 (2007).
39. S. Lagergren, *Kungliga Svenska Vetensk. Handl.*, **24**, 1 (1898).
40. Y. S. Ho and G. McKay, *Process Biochem.*, **34**, 451 (1999).
41. I. Mobasherpour, E. Salahi and M. Ebrahimi, *Res. Chem. Intermed.*, **38**, 2205 (2012).
42. I. Langmuir, *J. Am. Chem. Soc.*, **40**, 1361 (1918).
43. H. M. F. Freundlich, *Z. Phys. Chem.*, **57**, 385 (1906).
44. J. P. Hobson, *J. Phys. Chem.*, **73**, 2720 (1969).
45. K. Y. Foo and B. H. Hameed, *Chem. Eng. J.*, **156**, 2 (2010).
46. W. J. Weber and J. C. Morris, *J. Sanit. Eng. Div. Am. Soc. Civ. Eng.*, **89**, 31 (1963).
47. S. J. Allen, G. McKay and K. Y. H. Khader, *Environ. Pollut.*, **56**, 39 (1989).
48. K. P. Lisha, S. M. Maliyekkal and T. Pradeep, *Chem. Eng. J.*, **160**, 432 (2010).
49. H.-T. Fan, J.-B. Wu, X.-L. Fan, D.-S. Zhang, Z.-J. Su, F. Yan and T. Sun, *Chem. Eng. J.*, **198-199**, 355 (2012).
50. F. Boudrahem, F. Aissani-Benissad and A. Soualah, *J. Chem. Eng. Data*, **56**, 1804 (2011).
51. H.-T. Fan, Z.-J. Su, X.-L. Fan, M.-M. Guo, J. Wang, S. Gao and T. Sun, *J. Sol-Gel Sci. Technol.*, **64**, 418 (2012).